

## Calculation of Air Temperatures above the Urban Canopy Layer from Measurements at a Rural Operational Weather Station

BRUNO BUENO

*Massachusetts Institute of Technology, Cambridge, Massachusetts*

JULIA HIDALGO AND GRÉGOIRE PIGEON

*GAME/CNRM Météo-France and CNRS, Toulouse, France*

LESLIE NORFORD

*Massachusetts Institute of Technology, Cambridge, Massachusetts*

VALERY MASSON

*GAME/CNRM Météo-France and CNRS, Toulouse, France*

(Manuscript received 23 March 2012, in final form 31 July 2012)

### ABSTRACT

Urban canopy models (UCMs) are being used as urban-climate prediction tools for different applications including outdoor thermal comfort and building energy consumption. To take advantage of their low computational cost, UCMs are often forced offline without being coupled to mesoscale atmospheric simulations, which requires access to meteorological information above the urban canopy layer. This limits the use of UCMs by other scientific and professional communities, such as building engineers and urban planners, who are interested in urban-climate prediction but may not have access to mesoscale simulation results or experimental meteorological data. Furthermore, the conventional offline use of UCMs neglects the fact that the urban boundary layer can be affected by the surface and that the same forcing conditions may not be suitable for studying different urban scenarios. This paper presents a physically based and computationally efficient methodology to calculate forcing air temperatures for UCMs from meteorological data measured at operational weather stations. Operational weather stations are available for most cities in the world and are usually located in open areas outside the cities. The proposed methodology is satisfactorily evaluated against mesoscale atmospheric simulations and field data from Basel, Switzerland, and Toulouse, France.

### 1. Introduction

The urban heat island (UHI) effect, increase in air temperature observed in urban areas relative to the undeveloped rural surroundings (Oke 1987), can affect the energy performance of buildings (Bueno et al. 2012) and negatively influence the health and well-being of urban residents (Tan et al. 2010). The UHI effect is mainly caused by the different morphology of the urban terrain relative to the rural terrain, which has an impact on the

radiative budgets and the convective heat removal at the surface. Added to this is the lower evaporation due to the reduction of vegetated areas and the heat gain due to anthropogenic sources in cities.

Urban canopy models (UCMs) have been developed to represent urbanized surfaces in atmospheric numerical simulations and are being used as urban-climate prediction tools. The Town Energy Balance (TEB) scheme (Masson 2000) is a well-established example of a physically based UCM (Masson and Grimmond 2002; Lemonsu et al. 2004; Pigeon et al. 2008). These urban models can be coupled with a mesoscale atmospheric model (online approach) or forced with meteorological information above the urban canopy layer (offline approach) (Masson and Seity 2009). The offline approach

---

*Corresponding author address:* Bruno Bueno, Massachusetts Institute of Technology, 77 Massachusetts Ave., Cambridge, MA 02139.

E-mail: bbueno@mit.edu

takes advantage of the low computational cost of UCMs to effectively perform parametric analyses of urban design criteria. However, this approach generally assumes that forcing conditions are not affected by changes in the urban surface, which is a restrictive assumption if one is interested in contrasted scenarios of urban heat fluxes. Furthermore, forcing meteorological information above the urban canopy layer is only available through short-term experiments, a few permanent urban stations, and mesoscale atmospheric simulation results. This limits the use of UCM by other scientific and professional communities, such as building engineers and urban planners, who may be interested in urban-climate prediction but do not have access to this type of information. On the other hand, meteorological information can be easily found in weather data files obtained from measurements at operational weather stations, usually located in open areas outside the city (e.g., airports).

This paper presents a methodology to calculate forcing air temperatures for UCMs from meteorological information measured at operational weather stations. Other studies that calculate urban weather information through meteorological modeling can be found in the literature. Erell and Williamson (2006) presented a rural-to-urban weather transformation [the canyon air temperature (CAT) model] based on the local-scale urban meteorological parameterization scheme (LUMPS; Grimmond and Oke 2002), which requires the calibration of empirical parameters at the location of analysis. Based on similarity theory, Hidalgo et al. (2010) developed a correlation for the daytime UHI effect at mesoscale level under calm conditions. This correlation depends on the city size, the capping inversion height, and the urban–rural surface heat flux difference. Previously, Lu et al. (1997) had proposed an equivalent correlation for the nighttime case.

The methodology presented here is physically based and has a computational cost equivalent to UCMs. It integrates nighttime and daytime boundary layers and includes the wind impact. At each time step, an urban boundary layer (UBL) model calculates air temperatures above the urban canopy layer by solving an energy balance for a control volume inside the urban boundary layer. The model requires meteorological information measured at an operational weather station (air temperature at 2 m and wind speed at 10 m); surface sensible heat fluxes, which can be measured or provided by a UCM model and a soil–vegetation–atmosphere transfer (SVAT) model; and air temperatures at two different heights above the weather station provided by a vertical diffusion model (VDM). The VDM calculates vertical profiles of air temperature by solving a one-dimensional transient heat diffusion equation with the parameterizations

of Hong et al. (2006) and Louis (1979). The VDM requires measurements at the operational weather station and rural sensible heat fluxes.

This paper first describes the physics behind the UBL model and the VDM. Then, both models are evaluated separately by comparing them with three-dimensional high-resolution numerical simulations of an idealized city carried out with the Nonhydrostatic Mesoscale (Méso-NH) atmospheric model (Lafore et al. 1998). A second evaluation is presented by comparing the coupled VDM–UBL scheme with field data from the Basel Urban Boundary Layer Experiment (BUBBLE), carried out in Basel (Switzerland) in 2002 (Rotach et al. 2005), and the Canopy and Aerosol Particles Interactions in Toulouse Urban Layer (CAPITOU) experiment, carried out in Toulouse (France) during 2004 and 2005 (Masson et al. 2008). A discussion of the limitations and prospects of the proposed methodology is presented at the end.

## 2. Model description

The objective of this model is to describe the diurnal evolution of the UHI effect at mesoscale level based on an idealized conceptual model of rural and urban boundary layers as described in Hidalgo et al. (2010) (Fig. 1). At nighttime, rural and urban boundary layers usually have different stability regimes: the air is stratified at the rural site and mixed at the urban site. At daytime, the solar radiation heats the rural and urban surfaces and the atmosphere is well mixed up to a high altitude (Stull 1988). Additionally, the urban terrain delays the diurnal wave of air temperature because there is more surface exposed to the environment, increasing the effective thermal inertia (Erell and Williamson 2007). As a result, the UHI effect (urban–rural air temperature difference) presents a marked diurnal cycle with positive values at nighttime, negative values during the morning, and weak positive values during the afternoon (Oke 1987).

### a. Urban boundary layer model

The UBL model is based on an energy balance for a selected control volume inside the urban boundary layer delimited by the blending height  $z_b$ , at which the influences of individual obstacles on vertical profiles or fluxes become horizontally blended, and the boundary layer height  $z_i$  (Fig. 1). It differentiates between nighttime and daytime urban boundary layers and between the advection effect driven by a geostrophic wind (forced problem) and by the urban-breeze circulation (buoyancy-driven problem) (Hidalgo et al. 2008b).

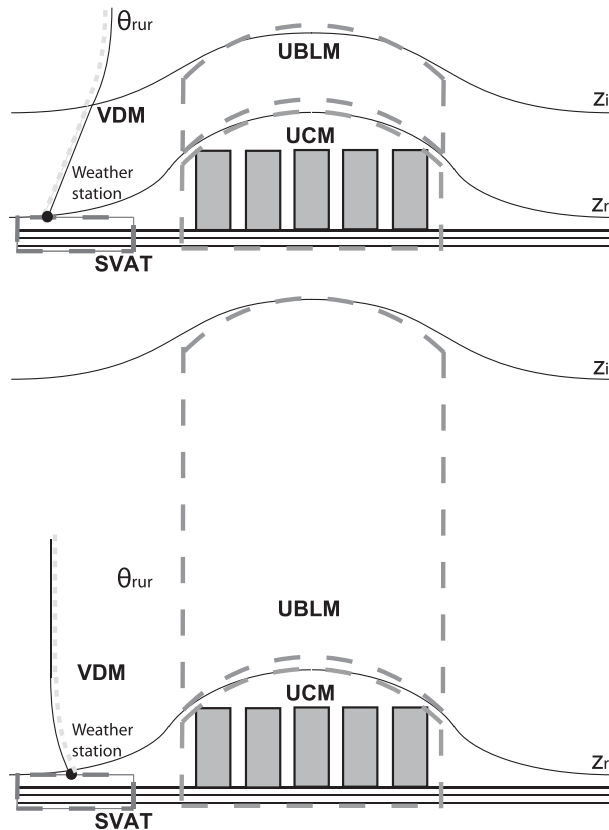


FIG. 1. Representation of a city and the physical domain of the VDM and the UBL model. Required surface heat fluxes can be measured or provided by a SVAT model and a UCM. Idealized nighttime and daytime vertical profiles of potential temperature are shown at rural and urban sites (not at scale). The characteristic height  $z_c$  is the canopy height between the ground and the height of obstacles;  $z_r$  is the blending height, at which the influences of individual obstacles on vertical profiles or fluxes become horizontally blended; and  $z_i$  is the boundary layer height.

The energy balance of the UBL model is expressed as

$$V_{CV}\rho c_v \frac{d\theta_{urb}}{dt} = H_{urb} + \int u_{ref}\rho c_p (\theta_{ref} - \theta_{urb}) dA_f, \quad (1)$$

where  $V_{CV}$  is the control volume,  $\rho$  is the air density,  $c_v$  is the air specific heat at constant volume,  $c_p$  is the air specific heat at constant pressure,  $\theta_{urb}$  is the average potential temperature of the control volume,  $H_{urb}$  is the sensible heat flux at the surface of the control volume (W),  $\theta_{ref}$  is a reference potential temperature outside the control volume,  $u_{ref}$  is a reference air velocity, and  $A_f$  is the lateral area of heat exchange between the control volume and its surroundings (see Table 1 for a description of all terms). In Eq. (1), the term on the lhs represents the thermal inertia of the control volume and the second term on the rhs represents the advection effect. The model assumes that the

TABLE 1. Nomenclature.

$A_{city}$	City horizontal area, $m^2$
$A_f$	Lateral heat exchange area, $m^2$
$c_p$	Air specific heat at constant pressure, $J\ kg^{-1}\ K^{-1}$
$c_v$	Air specific heat at constant volume, $J\ kg^{-1}\ K^{-1}$
$C_{vk}$	von Kármán constant
$dx$	Length of the control volume parallel to the main wind direction, m
$D$	City characteristic length, m
$E$	Turbulent kinetic energy, $m^2\ s^{-2}$
$g$	Gravity acceleration, $m\ s^{-2}$
$H_{rur}$	Rural sensible heat flux at surface W of control volume, $W\ m^{-2}$
$H_{urb}$	Urban sensible heat flux at surface W of control volume, $W\ m^{-2}$
$k_w$	Urban-breeze circulation scale constant
$K_d$	Diffusion coefficient, $m^2\ s^{-1}$
$l_k$	Length scale, m
$L$	Monin–Obukhov length, m
$P_{city}$	City perimeter, m
$Ri$	Richardson number
$t$	Time, s
$u_{circ}$	Urban-breeze circulation velocity, $m\ s^{-1}$
$u_{ref}$	Reference wind speed in the UBL model, zonal wind force in the mesoscale simulations, $m\ s^{-1}$
$u_{wind}$	Wind air velocity, $m\ s^{-1}$
$u_*$	Friction velocity, $m\ s^{-1}$
$V_{CV}$	Control volume, $m^3$
$w_s$	Mixed-layer velocity scale, $m\ s^{-1}$
$w_*$	Convective velocity scale, $m\ s^{-1}$
$W$	Width of the city orthogonal to the wind direction, m
$z$	Vertical space component, m
$z_c$	Canopy height, m
$z_i$	Boundary layer height, m
$z_{inv}$	Capping inversion height, m
$z_m$	Air velocity measurement height, m
$z_r$	Blending height, m
$z_{ref}$	Reference height at which temperature profiles are uniform, m
$z_0$	Roughness length, m
$\beta$	Buoyancy coefficient, $m\ s^{-1}\ K^{-1}$
$\Sigma H$	Difference between urban and rural sensible heat fluxes during one day of simulation, $W\ h\ m^{-2}$
$\delta$	Simulation time step, s
$\theta$	Potential temperature, K
$\rho$	Density, $kg\ m^{-3}$
$\phi_m$	Wind profile function

potential temperature is uniform inside the control volume and that there is no significant heat exchange at the top of it. The later assumption implies that the model neglects the longwave radiation exchange between the boundary layer air and the upper atmosphere and the entrainment of air at the top of the boundary layer. These effects are generally small and counteract each other.

At daytime, a control volume of the size of the city and height  $(z_i)_{day}$  is selected. The reference temperature of

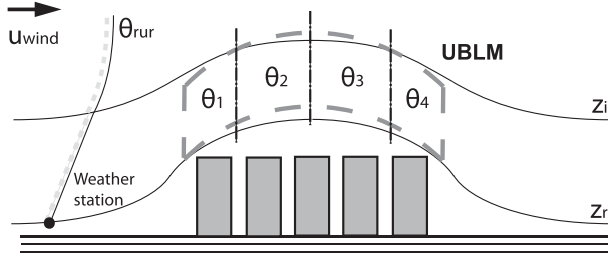


FIG. 2. Representation of the nighttime-forced scenario of the UBL model, in which the urban boundary layer is horizontally divided in various control volumes.

Eq. (1) is taken as the potential temperature outside the city at a height at which the vertical profile is considered uniform,  $\theta_{\text{rur}}(z_{\text{ref}})$ . This temperature is provided by the VDM.

In presence of geostrophic wind, the reference velocity is taken as the air velocity measured at the weather station  $u_{\text{wind}}(z_m)$  ( $z_m = 10$  m) and the lateral area of heat exchange  $A_f$  includes the width of the city orthogonal to the wind direction  $W$ . Under urban-breeze circulation at daytime, Hidalgo et al. (2010) proposed the following expression for the characteristic circulation velocity  $u_{\text{circ}}$ :

$$u_{\text{circ}} = k_w \left( \beta z_i \frac{H_{\text{urb}} - H_{\text{rur}}}{\rho c_p} \right)^{1/3}, \quad (2)$$

where  $k_w$  is a constant ( $k_w \sim 1$ ),  $\beta$  is the buoyancy coefficient ( $\beta = g\theta^{-1}$ ), and  $H_{\text{urb}}$  and  $H_{\text{rur}}$  are the sensible heat fluxes ( $\text{W m}^{-2}$ ) from the urban and the rural sites, respectively. The problem is assumed to be driven by buoyancy if the circulation velocity is greater than the air velocity measured at the weather station. For this situation, the circulation velocity [Eq. (2)] is used in the energy balance and the lateral area of heat exchange includes its entire perimeter  $P_{\text{city}}$ .

At night, in presence of geostrophic wind, the urban boundary layer is horizontally divided in various control volumes (Fig. 2). For the first control volume, the one upstream of the city, the reference potential temperature and wind velocity are assumed to have the following linear vertical profiles:

$$\theta_{\text{rur}}(z) = [\theta_{\text{rur}}(z_i) - \theta_{\text{rur}}(z_r)] \frac{z}{z_i} + \theta_{\text{rur}}(z_r) \quad (3)$$

and

$$u_{\text{wind}}(z) = u_{\text{wind}}(z_m) \frac{z}{z_m}, \quad (4)$$

TABLE 2. Surface coefficient  $C_{\text{surf}}$ , advection coefficient  $C_{\text{adv}}$ , and equivalent temperature  $\theta_{\text{eq}}$  used in Eq. (5) for each scenario. Here  $\theta_{\text{rur}}$  is the potential temperature outside the city at different heights ( $z_r$ ,  $z_i$ , and  $z_{\text{ref}}$ );  $\theta_{n-1}$  is the average potential temperature of the control volume upstream of the one considered;  $H_{\text{urb}}$  is the urban sensible heat flux ( $\text{W m}^{-2}$ ).

	$C_{\text{surf}}$	$C_{\text{adv}}$	$\theta_{\text{eq}}$
Night			
Forced (first)	$\frac{H_{\text{urb}}\delta}{z_i\rho c_v}$	$\frac{u_{\text{wind}}(z_m)z_i\delta c_p}{2z_m d x c_v}$	$\frac{2}{3}\theta_{\text{rur}}(z_i) + \frac{1}{3}\theta_{\text{rur}}(z_r)$
Forced (rest)			$\theta_{n-1}$
Buoyancy driven	$\frac{H_{\text{urb}}\delta}{z_i\rho c_v}$	$\frac{P_{\text{city}}u_{\text{circ}}\delta c_p}{A_{\text{city}}c_v}$	$\frac{1}{2}\theta_{\text{rur}}(z_i) + \frac{1}{2}\theta_{\text{rur}}(z_r)$
Day			
Forced	$\frac{H_{\text{urb}}\delta}{z_i\rho c_v}$	$\frac{Wu_{\text{wind}}(z_m)\delta c_p}{A_{\text{city}}c_v}$	$\theta_{\text{rur}}(z_{\text{ref}})$
Buoyancy driven	$\frac{H_{\text{urb}}\delta}{z_i\rho c_v}$	$\frac{P_{\text{city}}u_{\text{circ}}\delta c_p}{A_{\text{city}}c_v}$	$\theta_{\text{rur}}(z_{\text{ref}})$

where  $\theta_{\text{rur}}(z_r)$  is the air temperature measured at the weather station ( $z_r = 2$  m). The  $\theta_{\text{rur}}(z_i)$  is provided by the VDM, where the boundary layer height  $z_i$  is an input of the model. For simplicity, Eq. (4) assumes that the air velocity is 0 at  $z_r$ . For the control volumes downstream of the first one, the reference temperature is assumed to be uniform and given by the temperature of the control volume immediately upstream.

Under urban-breeze circulation at nighttime, the circulation velocity obtained by Eq. (2) is also used for the reference air velocity of Eq. (1), although this velocity scale was initially developed for daytime conditions [indeed, the circulation velocity scale proposed by Lu et al. (1997) for nighttime is equivalent to Eq. (2)]. The reference air temperature is assumed to have also a linear vertical profile [Eq. (3)].

To simplify the mathematical formulation of the UBL model, the height reference is taken at  $z_r$  [e.g.,  $(z_i)_{\text{model}} = (z_i)_{\text{real}} - (z_r)_{\text{real}}$  and  $(z_r)_{\text{model}} = 0$ ]. The numerical method used to solve Eq. (1) is implicit Euler, in which  $d\theta_{\text{urb}}/dt = (\theta_{\text{urb}} - \theta_{\text{urb}}^-)/\delta$ , where  $\delta$  is the simulation time step. Then, Eq. (1) can be expressed as

$$\theta_{\text{urb}} - \theta_{\text{urb}}^- = C_{\text{surf}} + C_{\text{adv}}\theta_{\text{eq}} - C_{\text{adv}}\theta_{\text{urb}}, \quad (5)$$

where  $C_{\text{surf}}$ ,  $C_{\text{adv}}$ , and  $\theta_{\text{eq}}$  are calculated for each scenario according to Table 2.

### b. Vertical diffusion model

The VDM calculates the vertical profiles of potential temperature above the weather station by solving the following heat diffusion equation:

$$\frac{\partial\theta(z)}{\partial t} = -\frac{1}{\rho(z)} \frac{\partial}{\partial z} \left[ \rho(z) K_d(z) \frac{\partial\theta(z)}{\partial z} \right], \quad (6)$$

where  $z$  is the vertical space component,  $\rho$  is the air density, and  $K_d$  is a diffusion coefficient. The lower boundary condition of Eq. (6) is the temperature measured at the weather station  $\theta(z_r)$ . The upper boundary condition accounts for the fact that at a certain height ( $z_{\text{ref}} \sim 150$  m), the profile of potential temperature is uniform and  $(\partial\theta/\partial z)_{z_{\text{ref}}} = 0$ .

The difficulty of calculating vertical temperature profiles through a diffusion equation lies in the calculation of the diffusion coefficient  $K_d$ . In some atmospheric models, such as the Méso-NH model, this coefficient is related to the turbulent kinetic energy (TKE) at each vertical level (Bougeault and Lacarrere 1989):

$$K_d = C_k l_k E^{1/2}, \quad (7)$$

where  $E$  is the TKE,  $C_k$  is a model parameter set equal to 0.4, and  $l_k$  is a length scale. In these models, a prognostic equation for the TKE is then solved as a function of the temperature and velocity fields (Martilli et al. 2002), so coupled equations for the air velocity components have also to be computed. This approach adds excessive complexity and computational cost to this particular application, in which the uncertainties associated with urban-climate prediction limit the reachable accuracy level. A simpler approach, proposed by Hong et al. (2006), calculates  $K_d$  based on correlations as a function of a mixed-layer velocity scale and the planetary boundary layer height, which has to be calculated iteratively.

The VDM proposes an alternative and robust solution, which combines the two approaches mentioned above. The diffusion coefficient is calculated by Eq. (7) and the TKE at each vertical level is approximated by

$$E = \max(w_s^2, E_{\text{min}}), \quad (8)$$

where  $w_s$  is the mixed-layer velocity scale and  $E_{\text{min}}$  is set equal to  $0.01 \text{ m}^2 \text{ s}^{-2}$ . Atmospheric models usually establish a minimum TKE given the difficulties of predicting very stable boundary layers (Bravo et al. 2008). A comprehensive description of the VDM is presented in the appendix.

### 3. Model evaluation

#### a. Comparison with mesoscale atmospheric simulations

This section presents a separate evaluation of the VDM and the UBL model through a comparison with idealized three-dimensional simulations carried out with

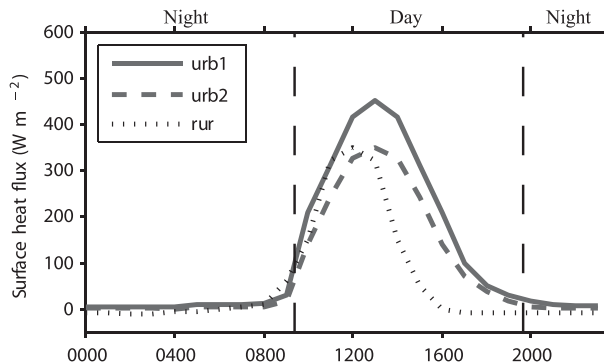


FIG. 3. Diurnal cycles of rural and urban sensible heat flux imposed in the mesoscale simulations for the cases of aggregated urban-rural difference  $\Sigma H = [1350 \text{ W h m}^{-2}$  (urb1) and  $650 \text{ W h m}^{-2}$  (urb2)]. The model considers daytime when  $H_{\text{urb}}$  reaches  $80 \text{ W m}^{-2}$  in the morning and nighttime when  $H_{\text{urb}}$  drops below  $30 \text{ W m}^{-2}$  in the afternoon.

the Méso-NH atmospheric model. The horizontal domain is  $80 \text{ km} \times 80 \text{ km}$  with a circular city in the middle ( $D = 10 \text{ km}$ ). The effects of the perturbations created by the city in the mean flow typically have a horizontal extent 2 to 3 times the size of the city (Hidalgo et al. 2008a), so the horizontal domain was large enough to prevent interferences from the cyclic boundary conditions. The horizontal grid resolution was set to  $500 \text{ m}$ . The vertical coordinate was composed of 56 levels over a vertical domain of  $4 \text{ km}$ . Vertical resolution varies from  $4 \text{ m}$  near the surface to  $250 \text{ m}$  on the top of the domain. The subgrid turbulence was parameterized following the scheme of Cuxart et al. (2000) and the mixing length of Bougeault and Lacarrere (1989).

Figure 3 shows the diurnal cycles of urban and rural surface heat fluxes imposed in the simulations, which represent typical scenarios observed in rural and urban areas. The integral of the difference between urban and rural sensible heat fluxes during one day of simulation ( $\Sigma H$ ), the capping inversion height  $z_{\text{inv}}$ , and the zonal wind force  $u_{\text{ref}}$  were used as external forcing parameters (the capping inversion height is the same as the boundary layer height at daytime). A set of these three parameters was chosen and fixed for each simulation. Simulations are carried out for  $\Sigma H = (1350 \text{ W h m}^{-2}$  and  $650 \text{ W h m}^{-2})$ ,  $z_{\text{inv}} = (1000 \text{ m}$  and  $1500 \text{ m})$ , and  $u_{\text{ref}} = (0 \text{ m s}^{-1}$ ,  $4 \text{ m s}^{-1}$ , and  $8 \text{ m s}^{-1})$ . The roughness length was set to  $z_{0r} = 0.01 \text{ m}$  for rural surfaces and  $z_{0u} = 1.0 \text{ m}$  for urban surfaces. The meteorological context was an idealized anticyclonic summer situation representative of southern France.

The simulation results used in this analysis correspond to a vertical plane passing through the city center. Rural conditions at different heights are taken as the

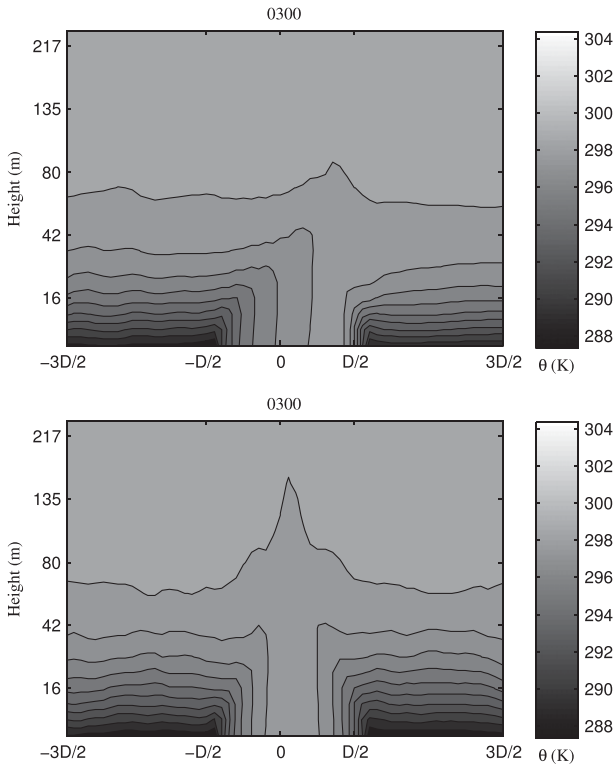


FIG. 4. Lower atmosphere nighttime contours of potential air temperature over a city of diameter  $D$  and its surroundings (top) in the presence of a geostrophic wind ( $u_{\text{ref}} = 4 \text{ m s}^{-1}$ ) and (bottom) under urban-breeze circulation ( $u_{\text{ref}} = 0 \text{ m s}^{-1}$ ) calculated by the mesoscale simulation for the case  $\Sigma H = 1350 \text{ W h m}^{-2}$  and  $z_{\text{inv}} = 1000 \text{ m}$ .

horizontal average of the mesh points contained in a line of length  $D$  centered on a distance  $D/2$  upwind of the city edge. Urban conditions are taken as the average of the mesh points contained in a plane of width  $D$  centered on the city center and height  $z_i$ .

Figure 4 shows the contours of potential temperature above and around the idealized city at nighttime. It can be seen that the urban boundary layer presents a horizontal distribution of air temperature due to the advection effect. Although this distribution could be captured by the discretization of the UBL model at nighttime (Fig. 2), in this study we are interested in the average air temperature above the city resulting from the average sensible heat flux over the city surface. It can also be noted that the effect of the heat source (the city) on the surface layer (first 15 m) is restricted to its horizontal area. This effect was already observed by Klysiak and Fortuniak (1999) and implies that, excluding microclimate effects, a weather station located outside and downstream of the city would measure similar conditions as one located upstream of the city. An asymmetrical urban boundary layer, typically observed

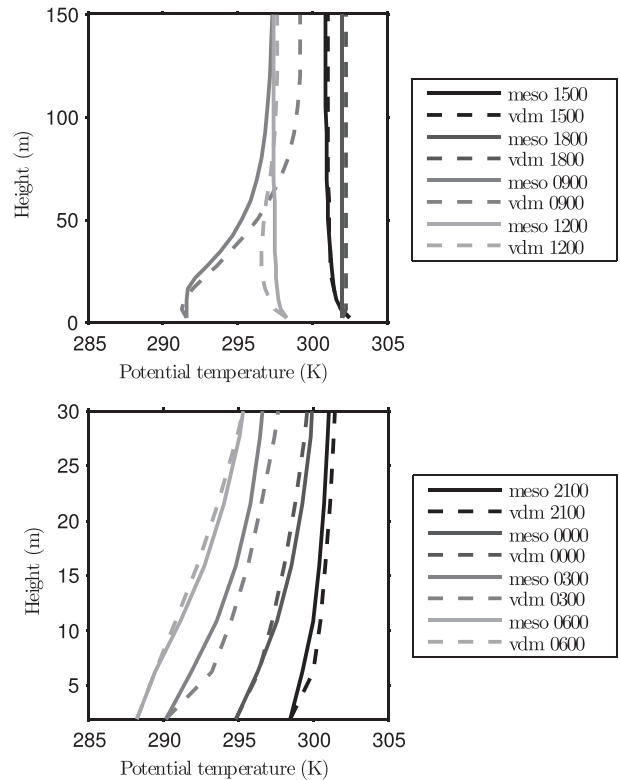


FIG. 5. Vertical profiles of potential temperature at (top) daytime and (bottom) nighttime calculated by the VDM and by the mesoscale simulations for the case  $\Sigma H = 1350 \text{ W h m}^{-2}$ ,  $z_{\text{inv}} = 1000 \text{ m}$ , and  $u_{\text{ref}} = 0 \text{ m s}^{-1}$ .

when the geostrophic wind is not negligible, may influence downstream rural areas but above the measurement height (2 m for temperature and 10 m for wind speed).

Figures 5 and 6 compare the vertical profiles of potential temperature at the rural site for different zonal wind forces. It can be seen that the VDM is able to reproduce the daytime and nighttime vertical distribution of potential temperature calculated by the mesoscale simulations. Some differences appear in the night-day transition period because of the different turbulence models used by the VDM and the Méso-NH model. The capacity of the VDM to predict  $\theta[(z_i)_{\text{night}}]$  and  $\theta[(z_{\text{ref}})_{\text{day}}]$ , which are the parameters required by the UBL model, is evaluated in Table 3. The root-mean-square error (RMSE) of  $\theta[(z_i)_{\text{night}}]$  and  $\theta[(z_{\text{ref}})_{\text{day}}]$  between the VDM and the mesoscale simulations ranges between 0.4 and 0.9 K, which is slightly lower than the error of the UBL model (Table 5).

The input parameters used by the UBL model for the comparison with mesoscale simulations are detailed in Table 4. The model requires rural air temperatures at three different heights  $\{\theta(z_r), \theta[(z_i)_{\text{night}}],$

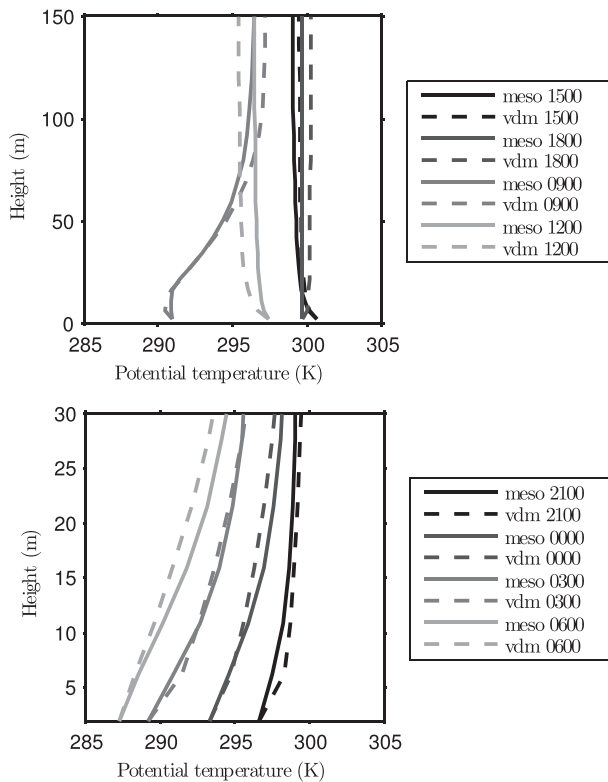


FIG. 6. As in Fig. 5, but for the case  $\Sigma H = 650 \text{ W h m}^{-2}$ ,  $z_{\text{inv}} = 1500 \text{ m}$ , and  $u_{\text{ref}} = 4 \text{ m s}^{-1}$ .

and  $\theta[(z_{\text{ref}})_{\text{day}}]$ , which are provided by the mesoscale simulation results at the rural site (for the purpose of this comparison since they are normally provided by the VDM). The same diurnal cycles of surface heat fluxes imposed to the mesoscale simulations are used in the UBL model (Fig. 3).

Figures 7 and 8 compare the average potential temperatures of the urban boundary layer calculated by the UBL model with the average urban and rural boundary layer temperatures calculated by the mesoscale simulation for different situations in terms of capping inversion height, surface heat flux, and zonal wind force. Differences in air temperature, computed as RMSE and mean-bias error (MBE) between the model and the mesoscale simulations, are presented in Table 5. The RMSE ranges between 0.6 and 1.0 K, where the daily maximum UHI effect calculated by the mesoscale model ranges between 1.8 and 2.5 K. Note that this UHI effect does not make use of the near-surface air temperature, which would come from an UCM. The MBE is generally low indicating that there are no systematic errors in the model.

The error of the VDM and the UBL model is related to their hypotheses and is acceptable given the important uncertainties associated with urban-climate predictions.

TABLE 3. RMSE and MBE between the potential temperature calculated by the VDM and by the mesoscale simulation at  $(z_i)_{\text{night}}$  and  $(z_{\text{ref}})_{\text{day}}$  for different zonal wind forces ( $u_{\text{ref}}$ ), aggregated surface heat fluxes ( $\Sigma H$ ), and capping inversion heights ( $z_{\text{inv}}$ ).

Mesoscale cases	$u_{\text{ref}}$ ( $\text{m s}^{-1}$ )	$z_{\text{inv}} = 1000 \text{ m}$ $\Sigma H = 1350 \text{ W h m}^{-2}$		$z_{\text{inv}} = 1500 \text{ m}$ $\Sigma H = 650 \text{ W h m}^{-2}$	
		RMSE (K)	MBE (K)	RMSE (K)	MBE (K)
$(z_i)_{\text{night}}$	0	0.6	0.3	0.4	-0.3
	4	0.9	0.5	0.5	-0.2
	8	0.8	0.3	0.7	-0.3
$(z_{\text{ref}})_{\text{day}}$	0	0.6	0.4	0.6	0.3
	4	0.6	0.5	0.7	0.4
	8	0.7	0.5	0.8	0.5

### b. Comparison with field data from Basel, Switzerland, and Toulouse, France

In this section, the VDM-UBL scheme is compared with field data from two boundary layer experiments: the intensive observational period (IOP) of the BUBBLE experimental campaign, carried out in Basel (Switzerland) between 10 June and 10 July 2002 (Rotach et al. 2005), and the CAPITOU experimental campaign carried out in Toulouse (France) from February 2004 to March 2005 (Masson et al. 2008).

In both experiments, weather data are measured simultaneously at rural and urban sites. At the urban sites, measurements include above-canopy air temperatures. The evaluation of the VDM-UBL scheme consists of introducing rural weather data as inputs in the model and comparing the calculated and observed forcing air temperatures above the urban canopy layer.

TABLE 4. Modeling inputs used in the comparison of the UBL model with mesoscale simulations. Other inputs of the model are rural air temperatures at three different heights  $\{\theta(z_r), \theta[(z_i)_{\text{night}}], \text{ and } \theta[(z_{\text{ref}})_{\text{day}}]\}$  and the wind speed at  $z_m$  calculated by the mesoscale simulation. The same diurnal cycles of rural and urban surface heat fluxes are imposed to the UBL model and to the mesoscale simulations.

Parameter	Settings
Simulation time step	300 s
Characteristic length of the city	$D, W = 10\,000 \text{ m}$
Perimeter of the city	$P_{\text{city}} = 4D$
Horizontal area of the city	$A_{\text{city}} = D^2$
Horizontal discretization for scenario night forced	$dx = D/4$
Nighttime boundary layer height	$(z_i)_{\text{night}} - z_r = 30 \text{ m}$
Daytime boundary layer height	$(z_i)_{\text{day}} = 1000 \text{ m}$
Reference height	$(z_{\text{ref}})_{\text{day}} = 150 \text{ m}$
Rural roughness length	$z_{0r} = 0.01 \text{ m}$
Circulation velocity coefficient	$k_w = 1.2$

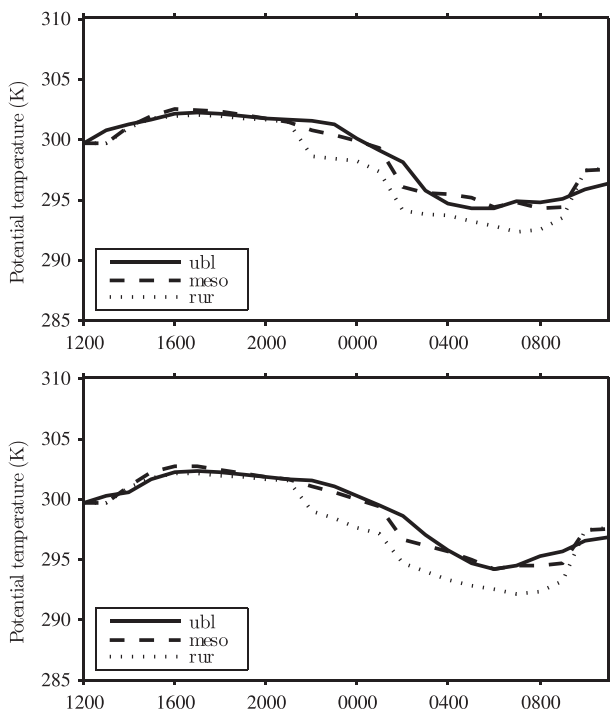


FIG. 7. Diurnal cycle of the average potential temperature over the urban boundary layer calculated by the UBL model and by the mesoscale simulation for the case  $\Sigma H = 1350 \text{ W h m}^{-2}$ ,  $z_{\text{inv}} = 1000 \text{ m}$ , and  $u_{\text{ref}} = [(\text{top}) 4 \text{ m s}^{-1}, (\text{bottom}) 0 \text{ m s}^{-1}]$ . The diurnal cycle of the average potential temperature over the rural boundary layer calculated by the mesoscale simulation is also represented (rur).

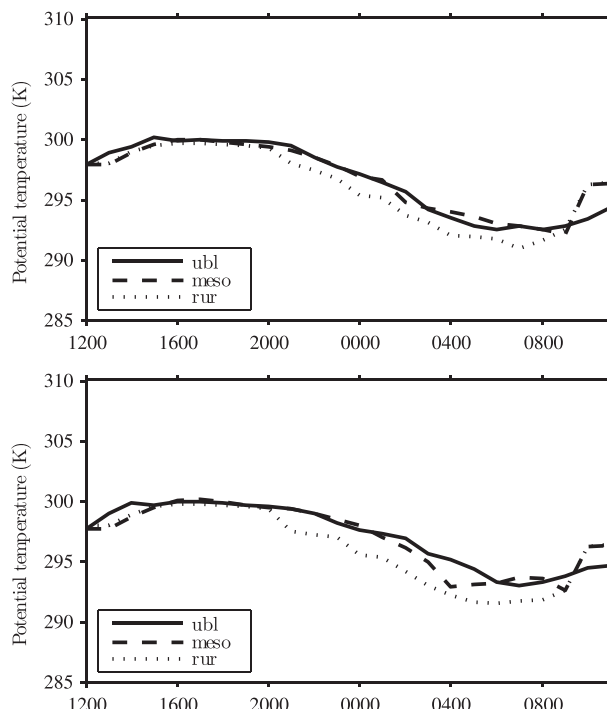


FIG. 8. As in Fig. 7, but for the case  $\Sigma H = 650 \text{ W h m}^{-2}$ ,  $z_{\text{inv}} = 1500 \text{ m}$ .

In addition, during the CAPITOUL experiment, radiosondes (Vaisala RS92) were launched from various rural and urban locations. As the balloons ascended, meteorological data were recorded each second. This led to a vertical resolution of approximately 5 m. In this analysis, the measurements from radiosondes launched at a rural site 17 km northwest from Toulouse are compared to the VDM.

From the network of weather stations of the CAPITOUL experiment, the station located at Mondouzil is assumed to be representative of rural conditions, and the station located next to the Monoprix building in the dense urban center of Toulouse is selected as representative of urban conditions.

The main urban experimental site in BUBBLE is Basel-Sperrstrasse. The site represents a heavily built-up part of the city center of Basel, mainly composed of residential buildings. The Grenzach weather station, inside the valley of the Rhine River, is used as the reference rural station.

Modeling input parameters are detailed in Table 6. City characteristic lengths of 7.5 and 5 km for Toulouse and Basel, respectively, are estimated based on aerial

views of the cities. Measured rural and urban sensible heat fluxes are imposed to the simulations.

Vertical profiles of potential temperature obtained with the VDM are compared with measurements from the radiosondes. Figure 9 compares calculated and measured vertical profiles for a day in winter and a day in summer, respectively. Given the simplicity of the VDM, the results show a reasonably good agreement with observations. The vertical shape of the profiles is reasonably well captured by the model, although the temperature values at the weather station, which are used as boundary conditions by the VDM, were not measured at the same location as where the radiosondes were launched.

The capacity of the VDM-UBL scheme to predict forcing air temperatures above the urban canopy layer is evaluated. Calculated monthly average diurnal cycles are compared with observations at the urban site for summer, fall, and winter in CAPITOUL (Fig. 10) and for summer in BUBBLE (Fig. 11). Air temperature measurements at 2 m at the rural site are also represented. As can be seen, the VDM-UBL scheme is able to capture both the UHI effect observed at night and the urban cool island (UCI) effect observed in the morning. Here, the UHI and UCI effects are defined as the difference between the forcing air temperatures



TABLE 5. RMSE and MBE between the average potential temperature of the urban boundary layer calculated by the UBL model and by the mesoscale simulation for different aggregated surface heat fluxes ( $\Sigma H$ ), capping inversion heights ( $z_{inv}$ ), and zonal wind forces ( $u_{ref}$ ). Errors are compared with the daily maximum urban–rural temperature difference calculated by the mesoscale simulation ( $UHI_{max}$ ).

Mesoscale cases $u_{ref}$ ( $m s^{-1}$ )	$z_{inv} = 1000$ m $\Sigma H = 1350 W h m^{-2}$			$z_{inv} = 1500$ m $\Sigma H = 650 W h m^{-2}$		
	RMSE (K)	MBE (K)	$UHI_{max}$ (K)	RMSE (K)	MBE (K)	$UHI_{max}$ (K)
0	0.6	0.1	2.4	1.0	0.1	2.4
4	0.8	0.0	2.5	0.9	−0.1	2.0
8	0.7	0.0	2.1	0.7	−0.1	1.8

above the urban canopy layer and the rural air temperature measured at 2 m.

Statistical results of this comparison are presented in Table 7. The RMSE between the model and observations ranges between 0.8 and 1.2 K for both experiments, where the average daily maximum UHI effect is 4.4 K in BUBBLE, 2.3 K in summer in CAPITOUL, and about 1.5 K in fall and winter in CAPITOUL. The MBE is generally small, which indicates that there are no systematic errors in the model.

A sensitivity analysis of the model indicates that values of  $(z_i)_{night}$  between 30 and 100 m and  $(z_i)_{day}$  between 800 and 2000 m have an impact of  $\pm 0.1$  K on the results.

#### 4. Conclusions

This paper presents a physically based and computationally fast two-model scheme to obtain forcing air temperatures above the urban canopy layer. The scheme requires meteorological information measured at an operational weather station and surface sensible heat fluxes at rural and urban locations. The vertical diffusion model

TABLE 6. Modeling inputs used in the comparison of the VDM–UBL scheme with field data from the experiment CAPITOUL. The scheme also requires  $\theta(z_r)$  and  $u(z_m)$  from measurements at the rural site. Here  $\theta[(z_i)_{night}]$  and  $\theta[(z_{ref})_{day}]$  are provided by the VDM to the UBL model. Rural and urban sensible heat fluxes are imposed from observations.

Parameter	Settings
Location	CAPITOUL: Toulouse BUBBLE: Basel
Characteristic length of the city	CAPITOUL: 7500 m BUBBLE: 5000 m
Simulation time step	300 s
Weather data time step	3600 s
Nighttime boundary layer height	$(z_i)_{night} - z_r = 50$ m
Daytime boundary layer height	$(z_i)_{day} = 1000$ m
Reference height	$(z_{ref})_{day} = 150$ m
Rural roughness length	$z_{0r} = 0.01$ m
Circulation velocity coefficient	$k_w = 1.2$

calculates vertical profiles of potential temperature at the rural site by solving a one-dimensional heat diffusion equation. The diffusion coefficient is calculated dynamically by approximating the TKE to the square of a mixed-layer velocity. Values of potential temperature at different heights calculated by the VDM are used in the urban boundary layer model, which calculates air temperatures above the urban canopy layer by applying an energy balance to the urban boundary layer (or subdivisions). The VDM–UBL scheme requires the rural and urban sensible heat fluxes calculated by the canopy models.

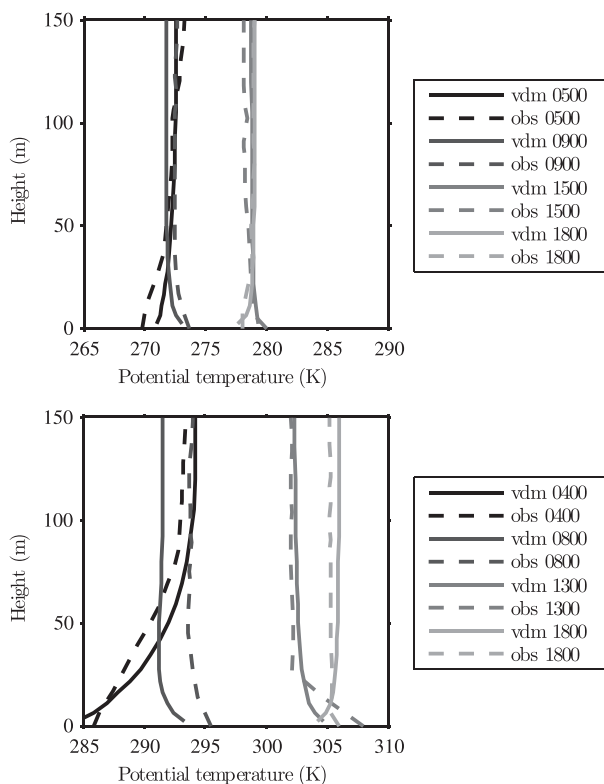


FIG. 9. Vertical profiles of potential temperature calculated by the VDM and observed during the CAPITOUL experiment on (top) 2 Mar 2005 and (bottom) 4 Jul 2004.

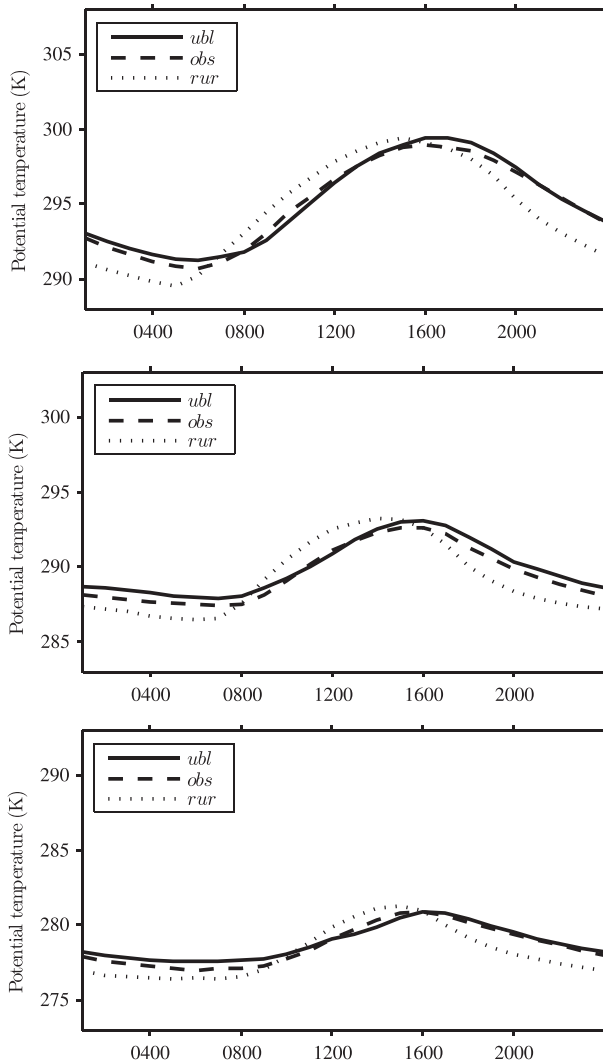


FIG. 10. Monthly average diurnal cycle of forcing air temperatures above the urban canopy layer calculated by the VDM-UBL scheme and observed during the CAPITOUL experiment for (top) July and (middle) October 2004, and (bottom) January 2005, in the dense urban area of Toulouse. Monthly average diurnal cycles of measured rural air temperatures (rur) for the same period are also represented.

The VDM-UBL scheme has been compared with three-dimensional mesoscale atmospheric simulations and with field data from the experiments BUBBLE (Basel, Switzerland) and CAPITOUL (Toulouse, France). The comparison shows a reasonable good agreement, given the important uncertainties associated with urban-climate predictions. The application of the proposed methodology has some restrictions in terms of the location of the reference weather station. This can be situated in any location in the periphery of the city as long as is not surrounded by urbanization and is not affected by site-specific microclimate conditions produced by the orography or by the presence of large bodies of water.

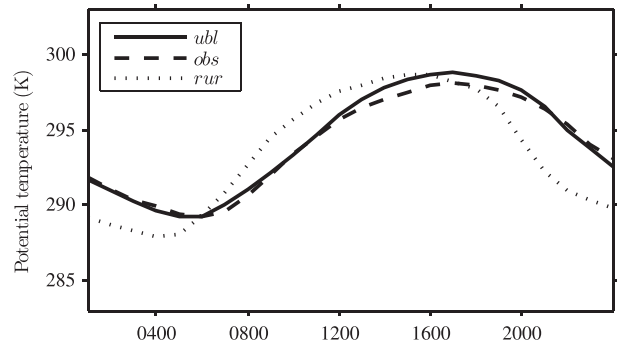


FIG. 11. Monthly average diurnal cycle of forcing air temperatures above the urban canopy layer calculated by the VDM-UBL scheme and observed during the BUBBLE experiment between 10 Jun and 10 Jul 2002. Monthly average diurnal cycle of measured rural air temperature (rur) for the same period is also represented.

The UBL model is being incorporated into the offline model of the Surface Externalisée (SURFEX) scheme (Masson et al. 2012) in the context of a French project of climate change impact on urban energy consumption [Modélisation Urbaine et Stratégies d'adaptation au Changement climatique pour Anticiper la Demande et la production Énergétique (MUSCADE); <http://www.cnrn.meteo.fr/ville.climat/spip.php?article85>]. This makes it possible to carry out long-term analyses of future climate scenarios without having to run computationally expensive mesoscale simulations. SURFEX is implemented with the urban canopy model TEB (Masson 2000), and the soil-vegetation-atmosphere transfer model Interactions between Soil, Biosphere, and Atmosphere (ISBA; Noilhan and Planton 1989). As an alternative to the VDM, this application uses an iterative procedure with the ISBA scheme to calculate air temperatures above the weather station (Lemonsu et al. 2013). The VDM-UBL scheme has been coupled with a

TABLE 7. RMSE and MBE between the forcing air temperatures above the urban canopy layer calculated by the UWG and observed during BUBBLE experiment between 10 Jun and 10 Jul 2002; and between the urban air temperatures calculated by the UWG and observed during CAPITOUL experiment in July and October 2004, and January 2005. Errors are compared with the average daily maximum UHI effect ( $\overline{UHI_{max}}$ ) observed during each period, defining the UHI effect as the difference between the forcing air temperatures above the urban canopy layer and the rural air temperature measured at 2 m.

Month	RMSE (K)	MBE (K)	$\overline{UHI_{max}}$ (K)
BUBBLE			
Summer	0.9	0.2	4.4
CAPITOUL			
Summer	0.8	0.2	2.3
Fall	1.1	0.4	1.5
Winter	1.2	0.2	1.4

SVAT model and a UCM to be used as an urban-climate prediction tool for the analysis and design of buildings and urban areas (Bueno et al. 2013).

*Acknowledgments.* This research was funded by the Singapore National Research Foundation through the Singapore–MIT Alliance for Research and Technology (SMART) Centre for Environmental Sensing and Modelling (CENSAM). Researchers from the GAME/CNRM (Météo-France, CNRS) were supported by the French National Research Agency (ANR) under Grant ANR-09-VILL-0003 and the Scientific Cooperation Foundation STAE in Toulouse in the context of the MUSCADE and the ACCLIMAT projects, respectively. We also thank Dr. Roland Vogt for sharing the BUBBLE data with us.

## APPENDIX

### The Vertical Diffusion Model

The length scale  $l_k$  used in Eq. (7) is determined by solving the following set of equations (Bougeault and Lacarrere 1989):

$$\int_z^{z+l_{\text{up}}} \beta[\theta(z) - \theta(z')] dz' = E(z), \quad (\text{A1})$$

$$\int_{z-l_{\text{down}}}^z \beta[\theta(z') - \theta(z)] dz' = E(z), \quad (\text{A2})$$

and

$$l_k = \min(l_{\text{up}}, l_{\text{down}}), \quad (\text{A3})$$

where  $l_{\text{up}}$  and  $l_{\text{down}}$  are the distances that a parcel originating from level  $z$ , and having the turbulent kinetic energy  $E(z)$ , can travel upward and downward before coming to rest because of buoyancy effects. The term  $l_{\text{down}}$  cannot be greater than the height above the ground.

The mixed-layer velocity used in Eq. (8) is calculated according to Hong et al. (2006):

$$w_s = (u_*^3 + \phi_m C_{\text{vk}} w_*^3 z/z_i)^{1/3}, \quad (\text{A4})$$

where  $u_*$  is the friction velocity,  $C_{\text{vk}} = 0.4$  is the von Kármán constant,  $\phi_m$  is a wind profile function,  $w_*$  is the convective velocity scale, and  $z_i$  is the boundary layer height.

For unstable and neutral conditions ( $H_{\text{rur}} > 0$ ), the wind profile function and the convective velocity scale are calculated as

$$\phi_m = \left(1 - 8 \frac{0.1z_i}{L}\right)^{-1/3}, \quad (\text{A5})$$

and

$$w_* = \left[\frac{g}{\theta(z_r)} \frac{H_{\text{rur}}}{\rho c_p} z_i\right]^{1/3}. \quad (\text{A6})$$

For stable conditions,  $w_* = 0$  and

$$\phi_m = 1 + 5 \frac{0.1z_i}{L}, \quad (\text{A7})$$

where  $L$  is the Monin–Obukhov length, calculated as

$$L = \frac{u_*^3 \theta(z_r) \rho c_p}{C_{\text{vk}} H_{\text{rur}}}. \quad (\text{A8})$$

The friction velocity  $u_*$  is calculated according to Louis (1979):

$$u_* = au(z_r) f_m^{1/2}, \quad (\text{A9})$$

where  $a = C_{\text{vk}}/\log(z_r/z_0)$  is a drag coefficient,  $u(z_r)$  is calculated from  $u(z_m)$  assuming a logarithmic profile, and  $f_m$  is a coefficient that accounts for the atmosphere stability and is given by

$$f_m = \frac{1}{(1 + 4.7\text{Ri})^2} \quad (\text{A10})$$

for stable and neutral conditions ( $\text{Ri} \geq 0$ ) and by

$$f_m = \frac{1 - 9.4\text{Ri}}{1 + c(-\text{Ri})^2} \quad (\text{A11})$$

for unstable conditions  $\text{Ri} < 0$ . In Eq. (A11), the constant  $c$  is given by  $c = 69.56a^2(z_r/z_0)^{1/2}$ , and the Richardson number is calculated as

$$\text{Ri} = \frac{gz_r[\theta(z_r) - \theta_{\text{soil}}]}{\theta(z_r)u(z_r)^2}. \quad (\text{A12})$$

## REFERENCES

- Bougeault, P., and P. Lacarrere, 1989: Parameterization of orography-induced turbulence in a mesobeta-scale model. *Mon. Wea. Rev.*, **117**, 1872–1890.
- Bravo, M., T. Mira, M. Soler, and J. Cuxart, 2008: Intercomparison and evaluation of MM5 and Meso-NH mesoscale models in the stable boundary layer. *Bound.-Layer Meteor.*, **128**, 77–101.
- Bueno, B., L. Norford, G. Pigeon, and R. Britter, 2012: A resistance-capacitance network model for the analysis of the interactions between the energy performance of buildings and the urban climate. *Build. Environ.*, **54**, 116–125.
- , —, J. Hidalgo, and G. Pigeon, 2013: The urban weather generator. *J. Build. Perform. Simul.*, doi:10.1080/19401493.2012.718797, in press.

- Cuxart, J., P. Bougeault, and J.-L. Redelsperger, 2000: A turbulence scheme allowing for mesoscale and large-eddy simulations. *Quart. J. Roy. Meteor. Soc.*, **126**, 1–30.
- Erell, E., and T. Williamson, 2006: Simulating air temperature in an urban street canyon in all weather conditions using measured data at a reference meteorological station. *Int. J. Climatol.*, **26**, 1671–1694.
- , and —, 2007: Intra-urban differences in canopy layer air temperature at a mid-latitude city. *Int. J. Climatol.*, **27**, 1243–1255.
- Grimmond, C. S. B., and T. R. Oke, 2002: Turbulent heat fluxes in urban areas: Observations and a local-scale urban meteorological parameterization scheme (LUMPS). *J. Appl. Meteor.*, **41**, 792–810.
- Hidalgo, J., V. Masson, and G. Pigeon, 2008a: Urban-breeze circulation during the CAPITOUL experiment: Numerical simulations. *Meteor. Atmos. Phys.*, **102**, 243–262.
- , G. Pigeon, and V. Masson, 2008b: Urban-breeze circulation during the CAPITOUL experiment: Observational data analysis approach. *Meteor. Atmos. Phys.*, **102**, 223–241.
- , V. Masson, and L. Gimeno, 2010: Scaling the daytime urban heat island and urban-breeze circulation. *J. Appl. Meteor. Climatol.*, **49**, 889–901.
- Hong, S.-Y., Y. Noh, and J. Dudhia, 2006: A new vertical diffusion package with an explicit treatment of entrainment processes. *Mon. Wea. Rev.*, **134**, 2318–2341.
- Klysisik, K., and K. Fortuniak, 1999: Temporal and spatial characteristics of the urban heat island of Lodz, Poland. *Atmos. Environ.*, **33**, 3885–3895.
- Lafore, J. P., and Coauthors, 1998: The Meso-NH atmospheric simulation system. Part I: Adiabatic formulation and control simulations. *Ann. Geophys.*, **16**, 90–109.
- Lemonsu, A., C. S. B. Grimmond, and V. Masson, 2004: Modeling the surface energy balance of the core of an old Mediterranean city: Marseille. *J. Appl. Meteor.*, **43**, 312–327.
- , R. Kounkou-Arnaud, J. Desplat, J.-L. Salagnac, and V. Masson, 2013: Evolution of the Parisian urban climate under a global changing climate. *Climatic Change*, **116**, 679–692.
- Louis, J.-F., 1979: A parametric model of vertical eddy fluxes in the atmosphere. *Bound.-Layer Meteor.*, **17**, 187–202.
- Lu, J., S. P. Arya, W. H. Snyder, and R. E. Lawson, 1997: A laboratory study of the urban heat island in a calm and stably stratified environment. Part I: Temperature field. *J. Appl. Meteor.*, **36**, 1377–1391.
- Martilli, A., A. Clappier, and M. W. Rotach, 2002: An urban surface exchange parameterisation for mesoscale models. *Bound.-Layer Meteor.*, **104**, 261–304.
- Masson, V., 2000: A physically-based scheme for the urban energy budget in atmospheric models. *Bound.-Layer Meteor.*, **94**, 357–397.
- , and C. Grimmond, 2002: Evaluation of the Town Energy Balance (TEB) scheme with direct measurements from dry districts in two cities. *J. Appl. Meteor.*, **41**, 1011–1026.
- , and Y. Seity, 2009: Including atmospheric layers in vegetation and urban offline surface schemes. *J. Appl. Meteor. Climatol.*, **48**, 1377–1397.
- , and Coauthors, 2008: The Canopy and Aerosol Particles Interactions in Toulouse Urban Layer (CAPITOUL) experiment. *Meteor. Atmos. Phys.*, **102**, 135–157.
- , and Coauthors, 2012: The SURFEXv7.2 land and ocean surface platform for coupled or offline simulation of Earth surface variables and fluxes. *Geosci. Model Dev. Discuss.*, **5**, 3771–3851.
- Noilhan, J., and S. Planton, 1989: A simple parameterization of land surface processes for meteorological models. *Mon. Wea. Rev.*, **117**, 536–549.
- Oke, T., 1987: *Boundary Layer Climates*. Methuen, 435 pp.
- Pigeon, G., M. A. Moscicki, J. A. Voogt, and V. Masson, 2008: Simulation of fall and winter surface energy balance over a dense urban area using the TEB scheme. *Meteor. Atmos. Phys.*, **102**, 159–171.
- Rotach, M. W., and Coauthors, 2005: BUBBLE—An urban boundary layer meteorology project. *Theor. Appl. Climatol.*, **81**, 231–261.
- Stull, R., 1988: *An Introduction to Boundary Layer Meteorology*. Kluwer Academic Publishers, 666 pp.
- Tan, J., and Coauthors, 2010: The urban heat island and its impact on heat waves and human health in Shanghai. *Int. J. Biometeor.*, **54**, 75–84.